A LUMINOUS RED NOVA IN M31 AND ITS PROGENITOR SYSTEM

S. C. Williams, M. J. Darnley, M. F. Bode and I. A. Steele
Astrophysics Research Institute, Liverpool John Moores University, IC2 Liverpool Science Park, Liverpool, L3 5RF, UK
Draft version April 30, 2015

ABSTRACT

We present observations of M31LRN 2015 (MASTER OT J004207.99+405501.1), discovered in M31 in January 2015, and identified as a rare and enigmatic luminous red nova (LRN). Spectroscopic and photometric observations obtained by the Liverpool Telescope showed the LRN becoming extremely red as it faded from its $M_V = -9.4 \pm 0.2$ peak. Early spectra showed strong Hα emission that weakened over time as a number of absorption features appeared, including Na I D and Ba II. At later times strong TiO absorption bands were also seen. A search of archival *Hubble Space Telescope* data revealed a luminous red source to be the likely progenitor system, with pre-outburst Hα emission also detected in ground-based data. The outburst of M31LRN 2015 shows many similarities, both spectroscopically and photometrically, with that of V838 Mon, the best studied LRN. We finally discuss the possible progenitor scenarios.

Subject headings: binaries: general — novae, cataclysmic variables — stars: individual (M31LRN 2015, V838 Mon) — stars: peculiar — supergiants

1. INTRODUCTION

Luminous red novae (LRNe) are a rare type of stellar transient typically more luminous than most novae, but fainter than supernovae (SNe), and characterized by a reddening color as they fade. The canonical system is V838 Monocerotis, which produced an outburst in early 2002, peaking at $M_V = -9.95$ (Munari et al. 2002b) and later generating a spectacular light echo (Bond et al. 2003). The only extragalactic red transient with a similar peak magnitude is M31-RV (Rich et al. 1989). Additionally, several other extragalactic transients show some similar properties to LRNe, but are significantly more luminous at peak (e.g. M85 OT2006-1, Kulkarni et al. 2007; PTF 10fqs, Kasliwal et al. 2011), and often grouped as intermediate luminosity red transients (ILRTs).

A number of mechanisms have been proposed to explain these events, including (1) a classical nova mechanism (Shara et al. 2010), (2) an unusual SN mechanism (e.g. Lovegrove & Woosley 2013), (3) giant planet capture (Retter & Marom 2003), (4) stellar mergers (Soker & Tylenda 2003) and (5) extreme AGB stars (Thompson et al. 2009). Kochanek (2011), in a study of ILRTs SN 2008S and NGC 300 OT2008, suggested that LRNe and ILRTs may have different physical origins, favoring the extreme AGB scenario as the likely mechanism for ILRTs. Tylenda et al. (2011) presented compelling evidence that V1309 Scorpii, a Galactic LRN, was a merger of a contact binary.

MASTER OT J004207.99+405501.1 (hereafter M31LRN 2015) was discovered on 2015 Jan 13.63 UT by the MASTER-Kislovodsk auto-detection system at $00^h42^m07^s.99$ $+40°55'01''.1$ (J2000) with an unfiltered magnitude of 19.0 (Shumkov et al. 2015b). The transient then brightened significantly from $R = 18.00 \pm 0.03$ on Jan 13.74 to $R = 16.82 \pm 0.02$ on Jan 14.71 (Ovcharov et al. 2015). A spectrum was taken by Ovcharov et al. (2015) on 2015 Jan 14.8, which revealed the presence of Hα emission, leading to the tentative classification of

the transient as a classical nova in M31.

As part of our extensive optical follow-up campaign for M31 novae (e.g. Shafter et al. 2011; Williams et al. 2014), we observed M31LRN 2015 photometrically and spectroscopically with the Liverpool Telescope (LT), a fully-robotic 2-meter telescope on the island of La Palma.

2. PHOTOMETRIC OBSERVATIONS

We obtained multi-color photometric observations of M31LRN 2015 using the IO:O CCD camera on the LT (Steele et al. 2004). Typically 3×120 s exposures were taken in each filter, which were decreased to 3×60 s at later times as M31 became more difficult to observe. The B, V and i'-band photometric data were calibrated using eight stars from Massey et al. (2006), with the i'-band magnitudes computed using transformations from Jordi et al. (2006). The z'-band data were calibrated using a single SDSS DR9 (Ahn et al. 2012) star (the only star in the field suitable for the calibration), J004225.86+405651.4, which may have affected the reliability, but by comparison to the i'-band photometry, we determined any systematic effect is small (< 0.1 magnitude). The photometry is presented in Table 1 and a light curve combining published data with those taken with the LT is shown in Figure 1.

The most striking feature of the light curve is the increasingly red color after peak, from $(B - i') = 0.650 \pm 0.007$ on Jan 19.89 to $(B - i') = 3.54 \pm 0.09$ on Mar 1.83. Our data imply optical peak was reached between 2015 Jan 19.89 and Jan 22.84. M31 has a distance modulus of $(m-M)_0 = 24.43 \pm 0.06$ (Freedman & Madore 1990). If we assume foreground reddening of $E_{(B-V)} = 0.062$ (Schlegel et al. 1998) and maximum total extinction at that position in M31 of $E_{(B-V)} = 0.18$ (Montalto et al. 2009), we conservatively assume that M31LRN 2015 was subject to reddening of $E_{(B-V)} = 0.12 \pm 0.06$. As such, the absolute peak magnitude of the transient was $M_V = -9.4 \pm 0.2$. It is possible that the peak magnitude was slightly brighter, although probably not significantly, given that the available photometric data in all

scw@astro.ljmu.ac.uk

Table 1
LT photometry of M31LRN 2015. BVi' calibrated against stars from Massey et al. (2006), z' calibrated against star from SDSS.

| Date (UT)	B	V	i'	z'
2015 Jan 17.87	16.172 ± 0.003	15.657 ± 0.002	15.463 ± 0.006	$\cdots$
2015 Jan 19.89	15.954 ± 0.004	15.459 ± 0.003	15.304 ± 0.006	$\cdots$
2015 Jan 22.85	15.965 ± 0.003	15.403 ± 0.002	15.198 ± 0.005	$\cdots$
2015 Jan 27.85	17.013 ± 0.008	16.080 ± 0.005	15.495 ± 0.006	$\cdots$
2015 Jan 30.88	17.431 ± 0.009	16.303 ± 0.004	15.542 ± 0.006	$\cdots$
2015 Feb 14.83	18.478 ± 0.029	16.720 ± 0.004	15.485 ± 0.006	15.230 ± 0.009
2015 Feb 26.84	19.178 ± 0.041	17.260 ± 0.011	15.649 ± 0.006	15.276 ± 0.015
2015 Mar 1.83	19.243 ± 0.088	$\cdots$	15.704 ± 0.009	15.248 ± 0.015
2015 Mar 6.83	$\cdots$	17.782 ± 0.036	15.854 ± 0.014	15.361 ± 0.023
2015 Mar 9.84	$\cdots$	$\cdots$	16.004 ± 0.017	$\cdots$
2015 Mar 12.83	$\cdots$	$\cdots$	16.121 ± 0.025	$\cdots$
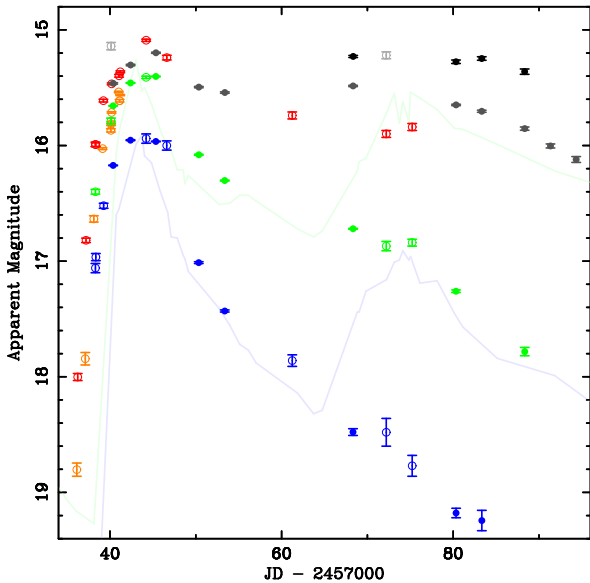
Figure 1. Light curve of M31LRN 2015 from LT observations (filled circles), as well as data from Ovcharov et al. (2015), Kurtenkov et al. (2015a,b), Shumkov et al. (2015a) and Fabrika et al. (2015) (all open circles). B-band data is represented by blue points; V, green; W, orange; R, red; I, light gray; i', dark gray; z', black. The light blue and green lines represent the B and V photometry respectively of the V838 Mon outburst from Munari et al. (2002b) shifted to the distance of M31 using a distance to V838 Mon of 6.1 kpc (Sparks et al. 2008) and the extinction of $E_{(B-V)} = 0.7$ (see Rushton et al. 2005).

filters seems to suggest a smooth transition from the rise to decline phases of the light curve.

3. SPECTROSCOPIC OBSERVATIONS

We obtained four spectra of M31LRN 2015 using the SPRAT spectrograph on the LT in red optimized mode, with a resolution of 18 Å, under photometric conditions. A spectrophotometric standard (Hiltner 600; Stone 1977) was observed on the night of 2015 Feb 4 in $1''.4$ seeing (FWHM) and used to flux calibrate the data. SPRAT has a fixed width slit equivalent to $1''.8$ on the sky. Seeing in the science spectra varies in the range $1''.5 - 2''.5$ (FWHM) between nights. This seeing variation forms the major cause of uncertainty in our absolute flux calibration, which we estimate as $\sim 25\%$. However since all observations were obtained with the slit aligned with the parallactic angle, the relative flux calibration within a single spectrum is better constrained (typically $< 10\%$ between 5000 and 7500 Å for all data).

The first spectrum was obtained on 2015 Jan 16.86, 3.2 days after discovery, and prior to peak. The only strong feature is the Hα emission, which has a FWHM of $900 \pm 100 \, \mathrm{km \, s^{-1}}$ and peaks at 6551.8 ± 0.5 Å, consistent with an M31 origin. We derive a Hα flux of $(7.8 \pm 0.7) \times 10^{-11} \, \mathrm{erg \, cm^{-2} \, s^{-1}}$ from the best-fit Gaussian profile. A small amount of Na I D absorption is detected (FWHM = $600 \pm 200 \, \mathrm{km \, s^{-1}}$), although this could be interstellar in origin, as well as Hβ being tentatively identified. This, along with the other SPRAT spectra taken of M31LRN 2015, is shown in Figure 2.

The second spectrum was obtained 17 days later on Feb 2.86. In this spectrum, the Hα flux had weakened to $(3.6 \pm 1.0) \times 10^{-11} \, \mathrm{erg \, cm^{-2} \, s^{-1}}$, the continuum is much redder, Na I D absorption is now strong and several other strong absorption features have emerged. The third spectrum, taken Feb 12.84, is somewhat similar, but Hα is now only just visible above the continuum (which is even redder). The most prominent absorption features in the second and third spectra are at 5882 ± 1 Å (Na I D; FWHM = $1000 \pm 200 \, \mathrm{km \, s^{-1}}$), 6131 ± 3 Å, 6240 ± 1 Å, and 6482 ± 1 Å. The 6482 ± 1 Å absorption line (FWHM = $900 \pm 200 \, \mathrm{km \, s^{-1}}$) is likely to be Ba II (6496.9 Å) blueshifted by $690 \pm 50 \, \mathrm{km \, s^{-1}}$, making the more poorly constrained 6131 ± 3 Å line consistent with Ba II (6141.7 Å). There is also a less prominent absorption feature blue-ward of Na I D with a minimum at 5841.6 Å, but a profile could not be fit, which is possibly caused by Ba II (5853.7 Å). The absorption at 6240 ± 1 Å, may be caused by Fe II, as seen (along with Ba II) in the V838 Mon spectra published by Goranskii et al. (2002). We estimate the Na I D equivalent width (EW) as 1.2 ± 0.3 Å on Jan 16.86 and 5 ± 1 Å on Feb 12.84. Using the relation from Poznanski et al. (2011), this gives a rough approximation of $E_{(B-V)} \sim 0.4$ on Jan 16.86 and $E_{(B-V)} \sim 2$ on Feb 12.84. Note however that those authors warn against using Na I D EW in low-resolution spectra to estimate absolute extinction, but it does at least show that the absorbing column may be increasing between the two epochs.

The fourth spectrum was taken Feb 28.85 and showed significant changes, with the spectrum now somewhat resembling that of a K or M-type supergiant. No significant Hα emission is detected and there are clear TiO absorption bands, with the Ba II and Na I D lines still present. A spectrum was also taken on Feb 25.84 but is not included as it was very similar to the one taken Feb 28, but noisier.
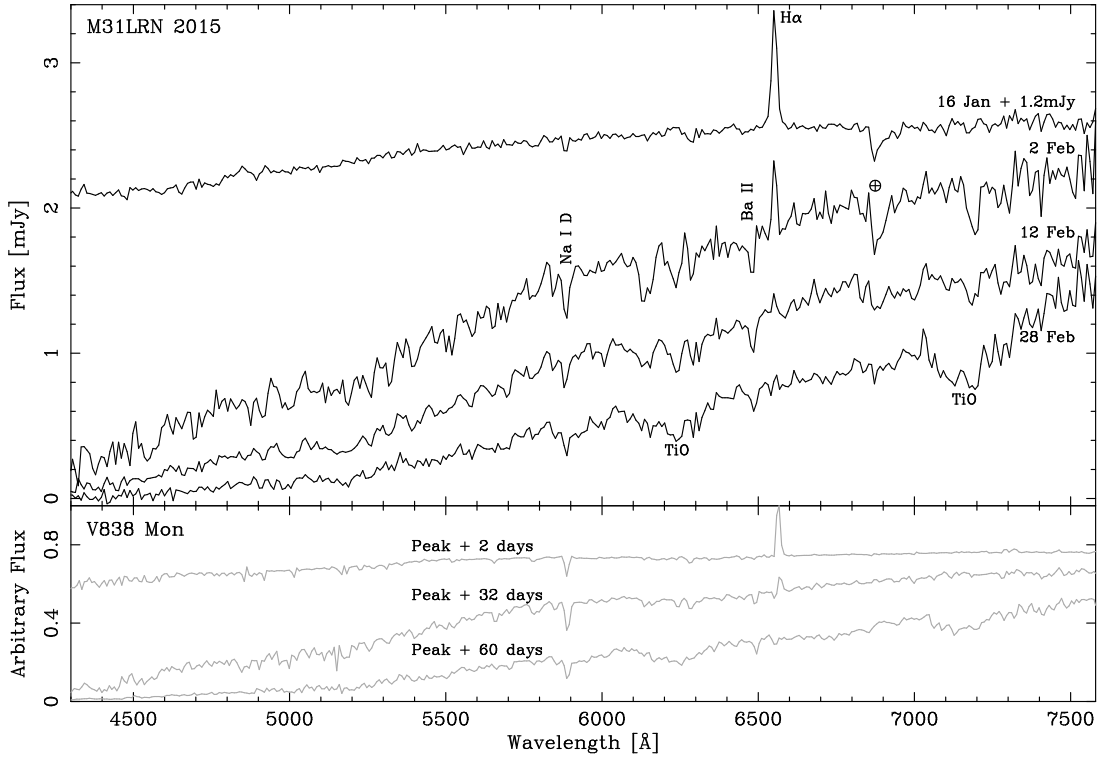
Figure 2. Top: The four LT SPRAT spectra of M31LRN 2015 taken 2015 Jan 16.86, Feb 2.86, Feb 12.84 and Feb 28.85, with peak occurring between 2015 Jan 19.89 and Jan 22.84 (see text). Bottom: Three spectra of V838 Mon from Rushton et al. (2005) with respect to its peak, binned to a similar resolution as our SPRAT spectra of M31LRN 2015.

4. THE PROGENITOR SYSTEM

Having successfully recovered a number of progenitor systems for M31 novae (Bode et al. 2009; Darnley et al. 2014; Williams et al. 2014), we used the same method to search for a possible progenitor system of M31LRN 2015. The archival *Hubble Space Telescope (HST)* observations were taken using the Advanced Camera for Surveys Wide Field Channel (ACS/WFC) through F555W and F814W filters on 2004 Aug 16.5 (prop. ID: 10273). Three i'-band LT frames taken on 2015 Jan 17.87 were stacked and 37 bright stars common to both observations were used to compute the geometric transformation between the two datasets using IRAF (Tody 1986) routines. This transformation was used to determine the position of the quiescent M31LRN 2015 in the archival *HST* data.

This analysis reveals a source within 1σ of the position of M31LRN 2015 in the *HST* data. Photometry was performed on all sources using DOLPHOT (v2.0[1]; Dolphin 2000). The closest source to the calculated position of M31LRN 2015, the progenitor candidate, is located at a distance of 0.55 ACS/WFC pixels, 0.5σ or $0\rlap{.}''027$, and has magnitudes of F555W $= 23.43 \pm 0.04$ and F814W $= 22.09 \pm 0.01$. We also note there is an additional source 1.4σ or $0\rlap{.}''077$ away. This second source has a magnitude of F814W $= 24.48 \pm 0.07$, but is undetected in the F555W data. The calculated position of M31LRN 2015, along with those nearby sources are shown in Figure 3. Using a similar method to that described in Williams et al. (2014), we determine the probability of a source being within $0\rlap{.}''027$ by chance is just 3%, given the resolved local stellar density.
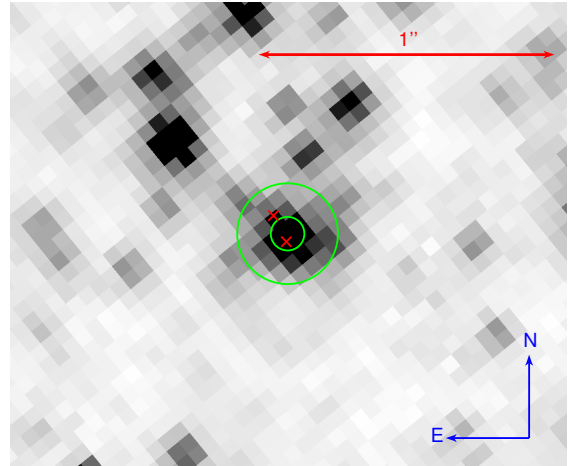
Figure 3. F814W *HST* (negative) image of the location of M31LRN 2015 taken 2004 Aug 16.5. The 1σ and 3σ errors on the calculated position of the quiescent system are represented by green circles. The red crosses represent the positions of the nearby sources in the *HST* data.

Employing the conversions from Sirianni et al. (2005) and using the distance and reddening towards M31LRN 2015 in M31 (see Section 2) we estimate the absolute magnitude of the progenitor candidate to be $M_V = -1.50 \pm 0.23$, $M_I = -2.55 \pm 0.13$ with $(V - I)_0 = 1.05 \pm 0.15$, consistent with a red giant.

The Local Group Galaxies Survey (LGGS; Massey et al. 2006) data reveal a nearby source, J004208.06+405501.7, at $V = 22.33 \pm 0.09$, $(B - V) = 0.75 \pm 0.17$, $(V - R) = 0.62 \pm 0.10$ and $(R - I) = 0.65 \pm 0.04$. While it would first appear that the

progenitor is brighter in the Massey et al. (2006) catalog, an inspection of the images reveals this source is in fact a blend of several of the stars visible in Figure 3, including the two brightest. A source is clearly visible at the position of M31LRN 2015 in the LGGS narrowband Hα data (taken 2002 Sep 11), but nothing is seen at this position in either the [O III] or [S II] data. To remove any contribution from continuum emission in these narrowband images we subtracted the scaled LGGS R-band image from both the Hα and [S II] images, and the scaled V-band image from the [O III] image. The scaling was calculated by determining a linear fit between the broadband and narrowband data using SExtractor (v2.19.5; Bertin & Arnouts 1996) photometry of ~ 20000 objects in each image. A clear source was seen in the continuum-subtracted Hα data, indicating a strong Hα excess in the spectrum of the pre-outburst M31LRN 2015. Azimlu et al. (2011), who also used the LGGS data, list it as an H II region (#1527 in their paper), with an estimated luminosity of $6 \times 10^{34} \, \mathrm{erg \, s^{-1}}$. If indeed this is a star forming H II region, the luminosity implies a star formation rate of $\sim 5 \times 10^{-7} \, \mathrm{M_\odot \, yr^{-1}}$ (using the conversion from Kennicutt 1998). A SN remnant origin for this emission seems unlikely, due to the lack of [S II] emission and the small size, which implies an age of less than a few hundred years. If this is not an H II region, the most likely source of the Hα emission is the progenitor system itself, either directly from the progenitor or a companion, or from a period of mass loss.

5. DISCUSSION

M31LRN 2015 is a luminous, red transient in M31, characterized by weakening Hα emission on an increasingly red continuum, with a number of absorption lines emerging after peak, including Na I D and Ba II, and TiO bands appearing at later times. Considering the spectroscopic and photometric evolution of the outburst we conclude that this object is a LRN in M31, a conclusion that Kurtenkov et al. (2015b) reached independently from their data. We now compare the properties of this system to those of other proposed LRNe and ILRTs.

The light curves of both LRNe and ILRTs are characterized by slow evolution (compared to most novae) and significant reddening as they fade. The light curves of LRNe V1309 Sco (Mason et al. 2010) and V838 Mon (Munari et al. 2002b) show the brightness quickly falling in the bluer filters, but plateauing in the red filters. The light curve of V4332 Sagittarii (another LRN; Martini et al. 1999) also shows this object to be reddening about two weeks after discovery, although there is no color information for the earlier periods. The only LRN that shows clear evidence of a significant multiple-peak light curve structure is V838 Mon. ILRTs are more luminous at peak than the LRNe discussed above and they also show different photometric evolution. The first ILRT discovered, M85 OT2006-1, shows a long plateau phase (~ 70 days), with relatively little color evolution until later times (Kulkarni et al. 2007). ILRT PTF 10fqs showed a plateau phase (~ 40 days), before rapidly reddening (Kasliwal et al. 2011), and NGC 300 OT2008 also shows no major optical color evolution until later times (Bond et al. 2009). Our observations show that M31LRN 2015 clearly resembles LRNe, rather than IL-

RTs, both in peak luminosity and light curve evolution. In the late-time M31LRN 2015 light curve (see Figure 1), the i'-band plateau appears to be ending, giving a plateau time of $40-50$ days. Comparing the plateau time and luminosity to the common-envelope event theoretical models of Ivanova et al. (2013, see their Figure 1), M31LRN 2015 is consistent with the model for a merger with ejecta mass of 0.1 $\mathrm{M_\odot}$, but is also consistent with an event where the entire envelope is ejected.

The spectra of LRNe and ILRTs do show similarities, with both types of object exhibiting strong Na I D absorption and narrow Hα emission, but they also appear to show some differences. Strong [Ca II] emission has been seen in several ILRTs (see e.g. Kasliwal et al. 2011), which is not the case for LRNe. Additionally, strong TiO absorption bands were seen at later times in LRNe V4332 Sgr (Martini et al. 1999) and V838 Mon (see e.g. Rushton et al. 2005). These were also seen in M31-RV (Rich et al. 1989). V838 Mon is the LRN with the best spectroscopic coverage, and the evolution of M31LRN 2015 seems to match that very well, for example, Ba II (6496.9 Å) appears between ~ 2 days prior to peak ($t \sim -2$ days; on 2002 Feb 5) and $t \sim +9$ days in V838 Mon (Goranskii et al. 2002), and also appears in M31LRN 2015 after peak. It can be seen from Figure 2 that our second and third spectra of M31LRN 2015 are remarkably similar to spectra taken around $t \sim +32$ days of V838 Mon published by Rushton et al. (2005), with our fourth spectrum of M31LRN 2015 similar to V838 Mon at $t \sim +60$ days.

The only significant differences between M31LRN 2015 and V838 Mon are the pre-outburst detections of the progenitor systems and the second bright peak in the light curve of the latter. The V838 Mon system contains a young main-sequence binary companion (Munari et al. 2002a). For the case of M31LRN 2015, we may again be seeing a binary companion, but at a more evolved stage, and depending on the mechanism, this may not represent different progenitor stars for the outbursts themselves. Notably, no young stellar population similar to the locale of V838 Mon was found to be coincident with M31-RV (Bond & Siegel 2006). If the giant planet capture mechanism was responsible for LRNe outbursts, this system (along with M31-RV) would represent the first (albeit indirect) detection of extragalactic planetary systems. While the detected progenitor candidate does not exclude a classical nova mechanism (Darnley et al. 2012; Williams et al. 2014) for M31LRN 2015, the presence of a high-mass main-sequence star in the V838 Mon system and the strong evidence for a stellar merger in the case of V1309 Sco appears to rule it out for those systems. The spectra are not consistent with a typical nova eruption, although Shara et al. (2010) offer an explanation for this. The strong evidence for the V1309 Sco outburst being caused by the merger of a contact binary (Tylenda et al. 2011) suggests that if a single progenitor mechanism is responsible for all LRNe, this is likely to be the stellar merger scenario. Dong et al. (2015) reported possible variability in M31LRN 2015 pre-outburst. As discussed in Section 4, using images taken under different conditions for such faint sources in crowded fields can significantly affect the photometry and the ground-based data is in fact a blend of a number of stars. However, if all the other stars remained constant the brightening they detect from $g \sim 22.6$ to $g \sim 20.8$ between 2009 and

2014 may indeed be significant.

6. CONCLUSIONS

In this Letter we have presented photometric and spectroscopic observations of M31LRN 2015, and a search for the progenitor system in broad and narrowband archival data. Here we summarize the main conclusions.

- We used the LT to photometrically and spectroscopically observe M31LRN 2015, which is a LRN peaking at an absolute magnitude of $M_V = -9.4 \pm 0.2$. It took several days to reach optical peak, with the optical colors becoming increasingly redder over the following weeks.

- The spectra are characterized by a reddening continuum, weakening Hα emission and emerging absorption features, including Na I D and Ba II. At later times TiO absorption bands are also seen. M31LRN 2015 shows a number of similarities with the spectra of other transients classified as LRNe, resembling V838 Mon particularly closely.

- The likely progenitor system has an absolute magnitude of $M_V = -1.50 \pm 0.23$ with $(V - I)_0 = 1.05 \pm 0.15$, although this could represent photometry of a more luminous companion star. Pre-outburst Hα emission is likely to be related to the progenitor system, either directly or the local environment.

- The nature of all of the LRN class of objects is still uncertain, but our observations of M31LRN 2015 and its likely progenitor system suggest that the mechanism(s) must produce very similar outbursts (in peak luminosity, timescale and outburst evolution), and possibly within differing stellar populations. If a single progenitor mechanism is responsible for all LRNe, the balance of evidence favors the stellar merger pathway.

Further observations, particularly of the post-outburst system, may yield further clues to the nature of M31LRN 2015 and the LRN class of objects in general.

REFERENCES

Ahn, C. P., Alexandroff, R., Allende Prieto, C., et al. 2012, ApJS, 203, 21
Azimlu, M., Marciniak, R., & Barmby, P. 2011, AJ, 142, 139
Bertin, E., & Arnouts, S. 1996, A&AS, 117, 393
Bode, M. F., Darnley, M. J., Shafter, A. W., et al. 2009, ApJ, 705, 1056
Bond, H. E., Bedin, L. R., Bonanos, A. Z., et al. 2009, ApJ, 695, L154
Bond, H. E., & Siegel, M. H. 2006, AJ, 131, 984
Bond, H. E., Henden, A., Levay, Z. G., et al. 2003, Nature, 422, 405
Darnley, M. J., Ribeiro, V. A. R. M., Bode, M. F., Hounsell, R. A., & Williams, R. P. 2012, ApJ, 746, 61
Darnley, M. J., Williams, S. C., Bode, M. F., et al. 2014, A&A, 563, L9
Dolphin, A. E. 2000, PASP, 112, 1383
Dong, S., Kochanek, C. S., Adams, S., & Prieto, J.-L. 2015, ATel, 7173
Fabrika, S., Barsukova, E. A., Valeev, A. F., et al. 2015, ATel, 6985
Freedman, W. L., & Madore, B. F. 1990, ApJ, 365, 186
Goranskii, V. P., Kusakin, A. V., Metlova, N. V., et al. 2002, Astronomy Letters, 28, 691
Ivanova, N., Justham, S., Avendano Nandez, J. L., & Lombardi, J. C. 2013, Science, 339, 433
Jordi, K., Grebel, E. K., & Ammon, K. 2006, A&A, 460, 339
Kasliwal, M. M., Kulkarni, S. R., Arcavi, I., et al. 2011, ApJ, 730, 134
Kennicutt, Jr., R. C. 1998, ARA&A, 36, 189
Kochanek, C. S. 2011, ApJ, 741, 37
Kulkarni, S. R., Ofek, E. O., Rau, A., et al. 2007, Nature, 447, 458
Kurtenkov, A., Ovcharov, E., Nedialkov, P., et al. 2015a, ATel, 6941
Kurtenkov, A., Tomov, T., Fabrika, E. A., et al. 2015b, ATel, 7150
Lovegrove, E., & Woosley, S. E. 2013, ApJ, 769, 109
Martini, P., Wagner, R. M., Tomaney, A., et al. 1999, AJ, 118, 1034
Mason, E., Diaz, M., Williams, R. E., Preston, G., & Bensby, T. 2010, A&A, 516, A108
Massey, P., Olsen, K. A. G., Hodge, P. W., et al. 2006, AJ, 131, 2478
Montalto, M., Seitz, S., Riffeser, A., et al. 2009, A&A, 507, 283
Munari, U., Desidera, S., & Henden, A. 2002a, IAU Circ., 8005, 2
Munari, U., Henden, A., Kiyota, S., et al. 2002b, A&A, 389, L51
Munari, U., Henden, A., Vallenari, A., et al. 2005, A&A, 434, 1107
Ovcharov, E., Kurtenkov, A., Valcheva, A., & Nedialkov, P. 2015, ATel, 6924
Perryman, M. A. C., & ESA, eds. 1997, ESA Special Publication, Vol. 1200, The HIPPARCOS and TYCHO catalogues. Astrometric and photometric star catalogues derived from the ESA HIPPARCOS Space Astrometry Mission
Poznanski, D., Ganeshalingam, M., Silverman, J. M., & Filippenko, A. V. 2011, MNRAS, 415, L81
Retter, A., & Marom, A. 2003, MNRAS, 345, L25
Rich, R. M., Mould, J., Picard, A., Frogel, J. A., & Davies, R. 1989, ApJ, 341, L51
Rushton, M. T., Geballe, T. R., Filippenko, A. V., et al. 2005, MNRAS, 360, 1281
Schlegel, D. J., Finkbeiner, D. P., & Davis, M. 1998, ApJ, 500, 525
Shafter, A. W., Darnley, M. J., Hornoch, K., et al. 2011, ApJ, 734, 12
Shara, M. M., Yaron, O., Prialnik, D., Kovetz, A., & Zurek, D. 2010, ApJ, 725, 831
Shumkov, V., Pruzhinskaya, M., Tiurina, N., et al. 2015a, ATel, 6951
Shumkov, V., Lipunov, V., Gorbovskoy, E., et al. 2015b, ATel, 6911
Sirianni, M., Jee, M. J., Benítez, N., et al. 2005, PASP, 117, 1049
Soker, N., & Tylenda, R. 2003, ApJ, 582, L105
Sparks, W. B., Bond, H. E., Cracraft, M., et al. 2008, AJ, 135, 605
Steele, I. A., Smith, R. J., Rees, P. C., et al. 2004, SPIE, 5489, 679
Stone, R. P. S. 1977, ApJ, 218, 767
Thompson, T. A., Prieto, J. L., Stanek, K. Z., et al. 2009, ApJ, 705, 1364
Tody, D. 1986, SPIE, 627, 733
Tylenda, R., Hajduk, M., Kamiński, T., et al. 2011, A&A, 528, A114
Williams, S. C., Darnley, M. J., Bode, M. F., Keen, A., & Shafter, A. W. 2014, ApJS, 213, 10